URBAN INTEGRATED METEOROLOGICAL OBSERVATIONS
Practice and Experience in Shanghai, China

by Jianguo Tan, Limin Yang, C. S. B. Grimmond, Jianping Shi, Wen Gu, Yuanyong Chang, Ping Hu, Juan Sun, Xiangyu Ao, and Zhihui Han

The Shanghai Urban Integrated Meteorological Observation Network (SUIMON) is introduced with examples of intended applications in this megacity.

The world's population exceeds 7 billion, with half living in urban areas (United Nations 2013). Current projections suggest that the global population will reach 8 billion in 2025, with nearly 5 billion living in urban areas. This increase has formed, and will inevitably produce, hundreds of large cities (>1 million population), megacities (>10 million population), and conurbations (or mega regions), most of which are coastal in developing countries. Urbanization brings not only people to cities but also capital, services, convenience, and benefits to economic production. At the same time, however, natural hazards and huge environmental pressures, including extreme weather (e.g., urban floods, heat waves) and environmental episodes (e.g., haze, photochemical pollution) can pose significant challenges for the crisis and risk management of these areas, the effects of which are often exacerbated by the decreased resilience and increased vulnerability associated with dense urban populations and infrastructure, intensive economic activities and climate change (Tang 2008).

Observations of atmospheric conditions and processes in urban areas are fundamental to understanding the interactions between the underlying surface and the weather/climate and improving the performance of urban weather, air quality, and climate models. Such observations also provide key information for end users (e.g., decision makers, stakeholders, public) for a myriad of applications [see, e.g., the range described by Dabberdt (2012)].

A number of major field campaigns in urban areas have been conducted in various parts of the world for different purposes (Table 1). These include short-term campaigns such as in the United States [e.g., URBAN 2000 (Allwine et al. 2002), Joint Urban 2003 (Allwine et al. 2004), Pentagon Shield (Warner et al. 2007), and Madison Square Garden (Hanna et al. 2006)] and Europe [e.g., Expérience sur Sites pour Contraindre les Modèles de Pollution Atmosphérique et de Transport d'Emission (ESCOMPTE) (Cros et al. 2004), Canopy

AFFILIATIONS: TAN, SHI, GU, CHANG, AO, AND HAN—Shanghai Institute of Meteorological Science, Shanghai, China; YANG, HU, AND SUN—Shanghai Meteorological IT Support Center, Shanghai, China; GRIMMOND—Department of Meteorology, University of Reading, Reading, United Kingdom

CORRESPONDING AUTHOR: Prof. Jianguo Tan, Shanghai Institute of Meteorological Science, 166 Puxi Road, Shanghai 200030, China
E-mail: jianguot@21cn.com

and Aerosol Particles Interactions in Toulouse Urban Layer (CAPITOUL) (Masson et al. 2008), Basel Urban Boundary Layer Experiment (BUBBLE) (Rotach et al. 2005), Dispersion of Air Pollutants and Penetration into the Local Environment (DAPPLE) (Arnold et al. 2004), and Regent's Park and Tower Environmental Experiment (REPARTEE) (Harrison et al. 2012)]. These studies have had many objectives, including a focus on near-surface turbulence characteristics, vertical structure of the entire urban boundary layer (UBL), and air pollution.

In addition, observational networks have been established to focus on urban weather research. One notable example is the Helsinki Testbed concerned with mesoscale weather forecasting and dispersion. This has involved model development and verification, demonstration of integration of modern technologies with complete weather observation systems, end user product development, and data distribution for the public and research community (Dabberdt et al. 2005; Koskinen et al. 2011). Other examples include the Houston Environmental Aerosol Thunderstorm

TABLE 1. Examples of comprehensive urban studies conducted since 2000, with the following aspects included: tracer (T), dispersion (D), air quality (AQ), meteorology (M), planetary boundary layer (PBL), urban energy balance (UEB), convective processes (CP), and mesoscale processes (MP).

Name	Where	When	T	D	AQ	M	PBL	UEB	CP	MP	Reference
(a) Short-term campaigns											
URBAN 2000	Salt Lake City, United States	Oct 2000	Y								Allwine et al. (2002)
Joint Urban	Oklahoma City, United States	Jul 2003	Y	Y		Y	Y	Y			Allwine et al. (2004)
Pentagon Shield	Washington, DC, United States	2004	Y	Y							Warner et al. (2007)
Madison Square Garden	Manhattan, New York City, New York, United States	2004, 2005	Y	Y							Hanna et al. (2006)
ESCOMPTE	Marseilles-Berre, France	Jun–Jul 2001		Y	Y	Y	Y	Y			Cros et al. (2004)
BUBBLE	Basel, Switzerland	1 year 2002	Y	Y		Y	Y	Y			Rotach et al. (2005)
DAPPLE	London, United Kingdom	May 2002– Jul 2006	Y	Y	Y	Y					Arnold et al. (2004)
REPARTEE	London, United Kingdom	Oct 2006, Oct/Nov 2007	Y	Y	Y	Y	Y				Harrison et al. (2012)
CAPITOUL	Toulouse, France	Feb 2004– Mar 2005	Y	Y	Y	Y	Y	Y			Masson et al. (2008)
HEAT	Houston, Texas, United States	Jul–Sep 2005			Y	Y			Y	Y	Orville et al. (2004)
TOMACS	Tokyo metropolitan area, Japan	Summers 2011–13					Y		Y	Y	Maki et al. (2012)
ClearfLo	London, United Kingdom	Jan–Dec 2012			Y	Y	Y	Y		Y	Bohnenstengel et al. (2015)
(b) Long term (>1 year continuous observations)											
METROS	Tokyo, Japan	2002–05					Y		Y	Y	Takahashi et al. (2009)
NYC mesonet	New York City, New York, United States	2003–present				Y			Y	Y	Reynolds (2014)
DCNet	Washington, DC, United States	2003–present	Y	Y							Hicks et al. (2012)
Helsinki Testbed	Helsinki, Finland	Jan 2005– present			Y		Y	Y		Y	Y	Dabberdt et al. (2005), Koskinen et al. (2011)
SUIMON	Shanghai, China	2000–present			Y	Y	Y	Y	Y	Y	This paper

Project (HEAT) (Orville et al. 2004), which aimed to determine the sources and causes for the enhanced cloud-to-ground lightning over Houston, Texas, and the Tokyo Metropolitan Area Convection Study (TOMACS), designed to better understand various mesoscale processes over the Tokyo metropolitan area (Maki et al. 2012). Most of the urban observation studies to date have been for short periods, for a relatively limited set of atmospheric and environmental conditions, rather than the full range that need to be understood for ongoing urban operations.

In 1872, Shanghai established a multifunction observatory, Xujiahui ("Zikawei" in Shanghai dialect), one of a small group of urban stations with long (>100 years) continuous records (Gherzi 1950). In 1958, weather stations were installed in the 10 rural counties of the province of Shanghai, extending the spatial dimension to about 30 km. The first dedicated urban meteorological observations in China were established in the downtown area of Shanghai in the 1970s–early 1980s. The >10 monitoring sites located over urban surfaces were used to investigate a wide range of urban effects (Zhou and Chow 1990) such as the warmer air temperatures [urban heat island (UHI)], humidity characteristics (wet or dry island), precipitation patterns, and the spatial variability of air quality—notably, the turbidity island (Zhou et al. 1991).

Today in Shanghai, there are a series of networks of different instrument types [e.g., automatic weather stations (AWS), weather radar, met towers, wind profilers, lightning mapping systems, remote sensing systems] that provide dense observations through a network of networks, referred to here as Shanghai's Urban Integrated Meteorological Observation Network (SUIMON). SUIMON covers the whole of the Shanghai metroplex and nearby seashores, which includes major transportation facilities—notably the Shanghai container port, the largest in the world—and Pudong International Airport. The objective of this paper is to introduce the characteristics,
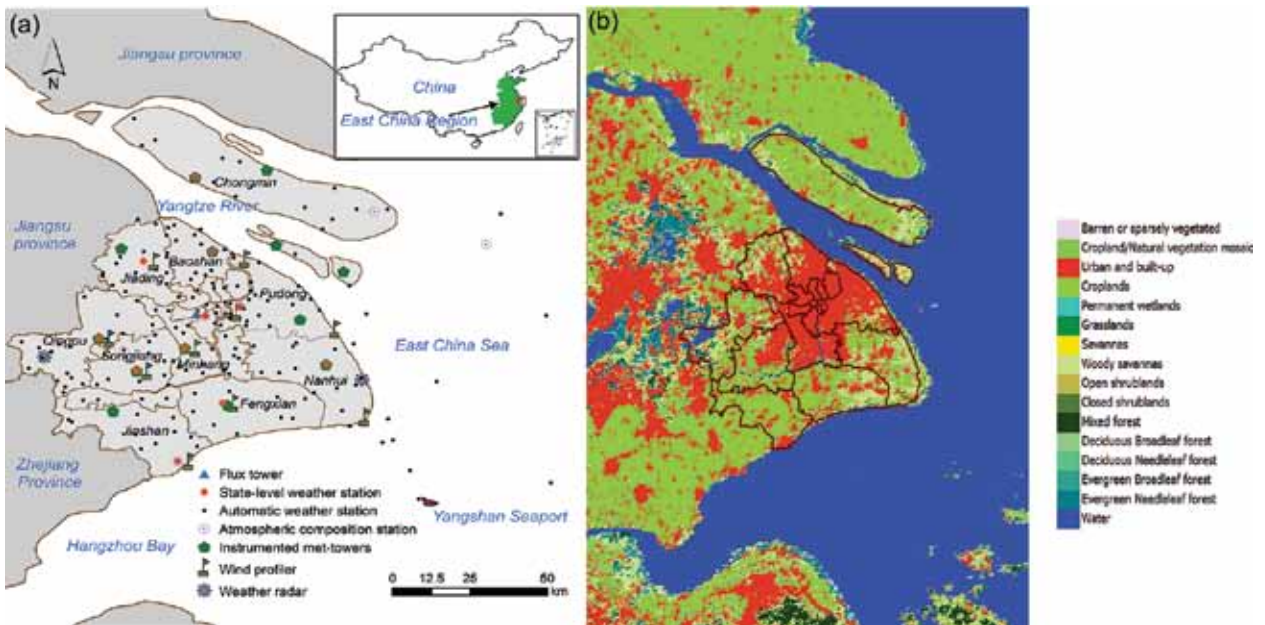
Fɪɢ. 1. (a) Shanghai's location within China (inset), observation sites within SUIMON in 2013. (b) The 10 counties that make up the province of Shanghai and the land cover derived from Landsat thermal mapper imagery (image date: 25 May 2010).

TABLE 2. Height distribution of Shanghai's buildings over eight stories in 2012 and 2000 (Shanghai Statistics Bureau 2014).

Type of building (stories)		8–10	11–15	16–19	20–29	>30	Total
Number of buildings	2012	4,367	15,125	7,484	3,839	1,207	32,022
	2000	536	684	831	1,266	212	3,529
Construction area (10^6 m^2)	2012	29.11	103.90	66.90	69.96	35.63	305.50
	2000	4.51	8.75	11.00	26.95	10.59	61.80

functions, and current state of SUIMON and to provide examples of intended applications and future plans for its development. This multifaceted network has the capability to cover many applications, while also providing opportunities for intensive campaigns with a rich spatial and temporal database to provide context. SUIMON already provides important data to support the economic activities within Shanghai and the East China region. For example, the world's largest seaport (Yangshan seaport; Fig. 1) is located on the coast here at the end of a chain of islands. A large amount of traffic travels along exposed roads to this destination. With a weather station located right at the container port, forecasts for both shipping and road traffic are supported. This allows both efficient loading of cargo and safer travel on both land and sea, under the wide range of meteorological conditions experienced in this region.

THE MULTIFUNCTION OF SUIMON.

Features of SUIMON. The coastal city of Shanghai, a direct-controlled municipality that is administratively equivalent to a province, is located at the middle of China's coastline (Fig. 1a), and had a population greater than 23 million in 2010 (Zou 2011), with more than 2.6 million automobiles, more than 32,000 tall buildings (>30 m tall), and over 1,200 skyscrapers

(>100 m tall) in 2012 (Table 2) (Shanghai Statistics Bureau 2014). The city, given its subtropical monsoon setting, with water on two of its three sides, frequently experiences typhoons, severe rain, heat waves, thunder and lightning, fog, storm surges, and other meteorological hazards.

To understand the interactions between the urban surface and atmospheric processes; improve the performance of urban weather, air quality, and climate models; and provide key information for city end users (e.g., decision makers, stakeholders, public), SUIMON has been established (see "SUIMON design features" for more information). The initial foci for SUIMON relate to high impact weather, urban environmental and micrometeorological conditions, and special needs for end users, along with data acquisition, integration, and assimilation systems. Of particular interest are rapidly changing atmospheric conditions associated with low pressure systems (e.g., severe convective weather) and more stagnant periods (e.g., fog and haze).

Today Shanghai's urban observations extend over an area (6,340 km²) that is roughly 120 km by 120 km (Fig. 1). SUIMON, a network of networks, has been established from different systems and instrumentation deployment types (Table 3). The ultimate goal of SUIMON is to provide measurements of all the processes that influence Shanghai's regional environment and the city itself, including both physical and chemical characteristics of the boundary layer and the free atmosphere, so linkages can be better understood.

Mega cities and conurbations have vast infrastructure—for example, transport networks, transmission lines, drainage networks, and underground spaces (e.g., metro lines, parking garages). These are all vulnerable to weather and can benefit from focused observations (Tang 2008). User-driven observations can provide the tailored, information-rich products and services that decision makers can use effectively. See the sidebar on "Examples of urban weather-sensitive applications in Shanghai" for examples delivered by SUIMON.

Some of the pressing air quality related scientific questions that are being addressed drawing on SUIMON relate to the temporal and spatial extent of the pollution plume from the Shanghai megapolis: how the photochemical processes function under very high aerosol loadings, the impact of the synoptic- and local-scale weather on pollutants, and the influence of atmospheric composition, especially ozone (O_3) and fine particles, on human health, agriculture, ecohydrology, and other systems.

With the development of SUIMON, and public environmental awareness of the data and

SUIMON DESIGN FEATURES

SUIMON is designed to satisfy the following features:
- Multipurpose: forecasts, research, service;
- Multifunction: high impact weather, urban environment, special end user needs;
- Multiscale: macro-/mesoscale, urban scale, neighborhood scale, street canyons, buildings;
- Multivariable: thermal, dynamic, chemical, biometeorological, ecological;
- Multiplatform: radar, wind profiler, ground-based, airborne, satellite based, in situ observation, sampling;
- Multilinked: linkages between all platforms;
with
- Management to facilitate exchange of data and information
- Ability to improve coordination of strategies and instruments and to identify gaps in observations based on science- and user-driven requirements
- Capability to intelligently combine observations from a variety of platforms using a data assimilation system that is tuned to produce the best estimate of the current state of the urban atmosphere

observational capability, the range of end users is increasing. These now include urban managers concerned with air pollution control and regulation and the public wanting information related to air quality. There is interest in real-time conditions and the forecast for the next few hours to days, tied to concerns about environmental exposure and its health effects. Other end users include those who need to aid decision making in an emergency response to nuclear, biological, or chemical (NBC) releases.

Observation networks within SUIMON. The locations of the stations within the networks of SUIMON were selected to provide spatial coverage across the Shanghai province while also considering siting requirements of the instruments used to undertake the observations. The finer details of exact locations are often constrained by logistics, such as access to sites or availability of land. As Shanghai is also rapidly changing, notably in terms of the rapid increase in tall buildings (Table 2), site characteristics also are rapidly changing. This impacts both the representativeness of individual sensors/sites and also end user needs, reflecting the increased density of people in certain areas. Thus, network design is an ongoing consideration. This is also tied closely to the quality assurance/quality control (QA/QC) that is undertaken within the data management system (DMS) that is central to SUMION (see next subsection).

A hierarchy of surface-level weather stations has been developed that include the World Meteorological Organization (WMO) official first order station (located at Baoshan) and nine weather stations (second order) across the province of Shanghai (Fig. 1a, Table 3). These 10 state-level weather stations meet standard WMO specifications (WMO 2008) and are maintained and supervised by Shanghai Meteorological Service (SMS) personnel. Each monitors meteorological elements automatically using an AWS. In addition, 65 automatic rain gauges and 200+ AWS stations monitor, at a minimum, temperature, humidity, precipitation, wind speed, and wind direction, sometimes with additional variables (e.g., air pressure, visibility), distributed across Shanghai at a range of different heights above ground level. These are used to characterize and validate thermodynamic and kinematic structures of various mesoscale features near the surface. Wind direction and wind speed, temperature, humidity, rain, and pressure are

EXAMPLES OF URBAN WEATHER-SENSITIVE APPLICATIONS IN SHANGHAI

In Shanghai, urban weather-sensitive applications include the following:

- Urban flood control: Flood control agencies need data on precipitation (rain, snow) distribution and runoff, as well as the water storage capability of urban pervious surfaces, drainage systems, and water-logged ground.
- Electric power: Power plants, grid operators, and local utilities need high-resolution air temperature for assessing energy demand and resulting loads on the electric grid. Wind and solar radiation are also needed for renewable energy assessments.
- Urban design: Urban planners and design departments need information on the UHI, vegetation stress index, urban air quality, and wind.
- Public health: Pollutant emissions and concentration, solar radiation, wind, humidity, and air temperature are needed at appropriate scales for street level, air quality, pollen, and predictions of heat stress.
- Transport management: Transport agencies need data on strong winds (especially channeling wind), precipitation and its forms (i.e., rain, freezing rain, sheet, or snow), surface state (dry, wet, ice covered), and high-resolution spatial forecasts (e.g., roadway scale) for metros, highways, and seaports.
- Security and emergency response: Urban emergency response agencies need timely and accurate information on extreme weather, such as detailed street-level flood information, and high spatial- and temporal-resolution wind, temperature, and moisture data in and above the urban canopy.

archived at the central database every 1 min. The overall density of surface-based temperature sensors across the 6340.5 km^2 area is about 1 per 30 km^2. The surface-based rain gauge networks are approximately 1 per 20 km^2.

A key characteristic of SUIMON is that the surface-based network is complemented with the capacity to observe the vertical characteristics of the atmosphere. This provides a four-dimensional dataset of the Shanghai area and the surrounding region, fulfilling a goal proposed for many urban areas (Grimmond et al. 2010; National Research Council 2010, 2012). At the WMO official first order station (Baoshan; Fig. 1) upper-air soundings provide vertical data (1-s temporal resolution) of temperature, humidity wind speed, and direction every 6 h. On the east coast and west Shanghai there are S-band Doppler Weather Surveillance Radar (WSR) systems (Table 3). These are supplemented by a moveable radar (X-band dual-polarization Doppler weather radar) to help

TABLE 3. Instrument types in SUIMON. Top table provides codes used in the main table.

*: Onsite personnel state-level weather station	F_{CO_2}: CO_2 flux	MS: Mean separation	SR: spatial resolution
Baoshan: 31.40 °N, 121.45°E	Freq.: frequency data are archived	N: number of stations providing data	ST: soil temperature
Dongtan: 31.52°N, 121.96°E	GRS: ground-based RS	NSMC: National Satellite Meteorological Centre	T: temperature
Expo park: 31.23°N, 121.5°E	GS: geostationary satellite	P: pressure	u, v, w: three-dimensional wind velocities
Pudong: 31.22°N, 121.55°E	Ht: height(s) sampled above the ground	PBL: planetary boundary layer	V: vertical
Qingpu: 31.13°N,121.12°E	IBT: instrumented broadcast tower	POS: polar-orbiting satellite	VP: vertical profile
Xujiahui: 31.19°N, 121.43°E	IT: instrument tower	Q*: net all-wave radiation	VT: virtual temperature
AEC: aerosol extinction coefficient	K↑: outgoing or reflected shortwave radiation	Q_E: latent heat flux	WD: wind direction
AOD: aerosol optical depth	K↓: incoming shortwave or solar radiation	Q_H: sensible heat flux	WS: wind speed
ASC: aerosol scattering coefficient	K↓: incoming direct solar radiation	R: resolution	WSR: Weather Surveillance Radar
AWS: automatic weather station	K_{DP}: specific differential phase shift	RH: relative humidity	Z_{DR}: differential reflectivity
BC: black carbon	L↑: longwave outgoing radiation	RS: remote sensing	λ: wavelength
CR: cover range	L↓: longwave incoming radiation	SO: surface observation	ϕ_{DP}: differential phase shift

Type	N	Coverage	Frequency	Variables	Model manufacturer (country)
SO*	10	MS: 25 km	1 min	T, P, RH, WS, WD, rain, visibility, ST	4: MILOS500 Vaisala (Finland), 6: ZQZ-CII Jiangsu Radio Scientific Institute Ltd. (China)
SO	1	Baoshan	1 min	$K{\downarrow}$, $K{\uparrow}$, $K{\downarrow}_{dir}$, Q*	FS-S6, FS-T1, FS-D1, Jiangsu Radio Scientific Institute (China)
SO, AWS^	200+	MS: 5.6 km	1 min	T, P, RH, WS, WD, rain, visibility (have four or more variables	Vaisala MAWS301, MilLOS500 (Finland), SAVVA-1(B), Jiangsu Radio Scientific Institute (China)
SO	65	MS: 4.8 km (plus AWS)	1 min	Rain	SR-II Shanghai Institute of Meteorological Science (China)
VP/IBT	13	MS: 22 km, Ht: 10^T, 30, 50, 70^T,100 m AGL	1 min	WS, WD [^{T}: T, RH]	ZQZ_TF Jiangsu Radio Scientific Institute (China), HMP45D Vaisala (Finland)
VP/RS wind	3	VR: 60 m (low mode), 60 m and 102 m (high mode) to 3000 m	30 min	Wind profiler: vertical and horizontal of WS, WD RASS: VT Qingpu	Vaisala LAP 3000 (Finland)
	7	VR: 60 m, MS: 25 km (plus LAP 3000)	30 min	Wind profiler: WS, WD	TWP3 Beijing METSTAR Radar CO. Ltd. (China)
VP/RS, upper-air sounding	1	Baoshan VR: per second, action distance: max 200 km; min: ≤100 m	6 h	Latitude, longitude, T, P, RH, WS, WD	L-band sounding system is composed of L-band secondary wind-finding radar; type GTS digital electronic radiosonde and ground check set. GFE(L)-I Nanjing DaQiao Machine CO., Ltd. (China)
WSR	2	λ: S-band fixed, CR: 230/460 km, E: east coast, W: western Shanghai	6 min	Radar reflectivity, radial velocity, spectrum width	WSR-88D (United States)[E], CINRAD WSR-98D (China)[W]
	1	λ: X-band, mobile CR: 120 km	6 min	Dual-polarization products (Z_{DR}, K_{DP}, ϕ_{DP})	DWSR-2001X-SDPIM (United States)
POS/RS	—	Overpass: 0900–1000, 1300–1400		AOD, profile of T, humidity, K and total radiance, total ozone	NSMC FY-3A, FY-3B (China), sensor: VIRR, IRAS, MWTS, MWHS, MERSI, MWRI, TOU, SBUS, SIM, ERM

Type	No.	Location / Details	Time	Parameter	Instrument
VP/RS	2	V: 10 km, R: 100/250 m, 1 operational, 1 movable	1 min	Vertical profile of temperature, humidity, water vapor density, liquid water content	TP/WVP: microwave radiometer 3000, Radiometrics (United States)
GPS-Met	31 (19 + 12)	MS: 14 km	30 min	Precipitable water vapor (PWV)	19 Trimble NetRs (United States), 12 Ashtech Z-12 (United States)
IT/Flux	1	Xujiahui, Ht: 80 m (building + tower height: 55 + 25 m)	10 Hz, 30 min	Q_H, Q_E, F_{CO2}, u, v, w, VT $K\downarrow$, $K\uparrow$, $L\downarrow$, $L\uparrow$, Q^*, T, RHWS,WD	Irgason Campbell Scientific (United States), CNR4 Kipp and Zonen (Netherlands), HMP155A Vaisala (Finland), ZQZ_TF Jiangsu Radio Scientific Institute (China)
SO/O₃	10	MS: 25 km, Ht: Xujiahui 55 m, others <15 m	1 min	Ozone analyzer: O_3	EC9810, Ecotech Inc. (Australia)
SO/NOx	10	MS: 25 km, Ht: Xujiahui 35 m, others <15 m	1 min	NO/NO₂/NO$_x$ analyzer: NO, NO₂, NO$_x$	EC9841B, Ecotech Inc. (Australia)
SO/SO₂	2	Ht: Expo park 4 m, Dongtan 5 m	1 min	SO₂ analyzer: SO_2	EC9850, Ecotech Inc. (Australia)
SO/CO	3	Ht: Xujiahui 55 m, Pudong 14 m, Dongtan 5 m	1 min	CO analyzer: CO	EC9830, Ecotech Inc. (Australia)
SO/VOCs	10	Ht: 2 m, campaigns on typical day at 10 stations	1 day	VOCs concentrations	Sample canister: 6 L silonite canister with silonite coated valve, 29-10622 Entech Instruments Inc. (United States), Laboratory Analysis: 7100 VOC preconcentrator Entech Instruments Inc. (United States), Agilent GC6890 gas chromatography coupled to Agilent MSD5975 N mass-selective detection (length: 60 m, diameter: 0.32 mm, film thickness: 1.0 μm)
SO/PM	3	Ht: Expopark, Pudong, Dongtan <10 m	1 min	PM_{10}, $PM_{2.5}$, PM_1	GRIMM180, GRIMM Technologies, Inc.(Germany)
SO/ASC	3	Ht: Expo park 4 m, Pudong 14 m, Dongtan 5 m	1 min	Nephelometer: ASC	M9003, Ecotech Inc. (Australia)
SO/BC	2	Ht: Pudong 14 m, Dongtan 5 m, λ: 370, 470, 520, 590, 660, 880, 950 nm	2 min	Aethalometer: BC light absorption by suspended aerosol particles	AE 31 Magee Scientific (United States)
GRS/AOD	3	Ht: Expo park 4 m, Pudong 14 m, Dongtan 5 m, λ: 1020, 936, 870, 670, 500, 440, 380, 340 nm	1 min	AOD, Angstrom index	CE318 sun photometer CIMEL (France)
VP/O3	1	Baoshan VR: per second	typical day	O_3 concentration profile	O₃-GPS sounding (China)
VP/GRS	3	2-fixed: Expo park, Baoshan; 1-movable VR: 5 or 10 m, from 90 m to 7 km	16 s	Ceilometer: PBL height, Vertical distribution of aerosols, Cloud base, AEC	CL31/CL51,Vaisala (Finland)
VP/GRS	2	Expo park, Pudong VR: 15, 30, 60, 75 m, from 100 m to 20 km	30 s	Vertical distribution of aerosols, PBL height	Micropulse lidar MPL-4B-IDS, SigmaSpace (United States)
POS/RS	—	Overpass: 2 times a day, λ: 5 bands, SR: 1 km		Cloud, surface temperature, soil moisture fog, haze	NOAA-15/-16/-17/-18 (United States)
POS/RS	—	Overpass: 1030 (T) 1330 (A) every 8 days, λ: 0.4–14.4 μm (36 bands), SR: 2 bands at 250 m, 5 at 500 m, 29 at 1 km		Surface temperature, cloud temperature, water vapor, ozone emissivity, surface reflectance, albedo, vegetation indices, land-cover type	National Aeronautics and Space Administration (NASA) MODIS EOS Terra and Aqua (United States)
GS/RS	—	SR 1.25 km, λ: 5 bands (1 VIS, 1 vapor, 3 IR)		Cloud, surface temperature, fog, haze	NSMC FY-2D, FY-2E, FY-2F (China)
GS/RS	—	λ: 0.55–4.0 μm (5 bands), SR: VIS band at 1 km, IR1–IR4 4 bands: at 4 km		Cloud, surface temperature, rain, fog, haze	MTSAT-2 (Japan)
GRS, lightning mapping	3	Locational accuracy: ~500 m CR: 200 km	1 s	Cloud-to-ground (CG) flashes and strokes survey-level cloud	Vaisala LS7000 (Finland)
GRS, lightning mapping	1	Locational accuracy: ~500 m CR: 200 km	1 s	Total cloud discharges, CG flashes and strokes	Vaisala LS8000 (Finland)

identify severe weather and estimate precipitation rates. Single- and dual-Doppler wind field retrieval technologies are used to identify boundary convergence lines (Liang 2007). The routine S-band radars provide total coverage of Shanghai municipality and neighboring Jiangsu and Zhejiang provinces with a temporal resolution of 6 min.

The lightning mapping system, including three LS7000 sensors and one LS8000 sensor (Table 3) covering the whole Shanghai and neighboring areas, provides continuous monitoring of intra- (and inter-) cloud and cloud-to-ground lightning density. Water vapor content is observed with a dense network of GPS-Meteorological Observing Systems project (GPS-Met) stations that consist of 31 receiving stations within Shanghai with a spatial resolution of 10–15 km. Beyond the radio soundings, two microwave radiometers (Table 3)—one operational and one movable—monitor the profile of temperature, humidity, water vapor density, and liquid water content to about 10 km, with a vertical resolution of 100 m from 250 m to 2 km and 250 m above (Table 3).

A network of 13 instrumented broadcasting masts (Fig. 1), with wind sensors at 10, 30, 50, 70, and 100 m above ground level (AGL), plus temperature and humidity sensors at 10 and 70 m AGL, provide vertical information close to the surface (lower boundary layer) (Fig. 2a). Ground-based remote sensing includes 10 wind profilers (Table 3) that provide detailed information about boundary layer wind fields and mixing layer height (Fig. 2b). These provide information from 60 to 3000 m with gates of 60 m or about 100-m resolution that vary with model and operating mode (high or low) across the network.

Local-scale flux measurements (Table 3) are conducted within the densely built-up area of Xujiahui (Fig. 1). Within the footprint of the flux tower is the site where routine weather data have been collected for more than 140 years. The micrometeorological instrumentation, mounted at 80 m, includes eddy covariance measurement (Aubinet et al. 2012) of turbulent sensible and latent (water vapor) heat plus carbon dioxide fluxes. Simultaneously the four components of net all-wave radiation (longwave and shortwave incoming and outgoing/reflected radiation) with slow response air temperature and relative humidity sensors are measured. With the flux measurements, the surface energy balance and carbon fluxes are being investigated (X.-Y. Ao et al. 2014, unpublished manuscript). These measurements will be used to verify and modify urban land surface models used in weather and the climate prediction model. Within Shanghai, radiation measurements are also undertaken in Baoshan (Table 3).

In addition to the physical characteristics of the atmosphere, observations related to atmospheric composition [e.g., ozone (O_3) and its precursors, aerosols] are measured at 10 sites (Fig. 1) across the region. As ground-level O_3 is formed as a result of complex photochemical reactions of nitrogen oxides, carbon monoxide (CO), and various volatile organic compounds (VOCs), the concentration of O_3 and its precursors are measured nearly 10 m above the surface (Table 3). VOCs concentrations sampled
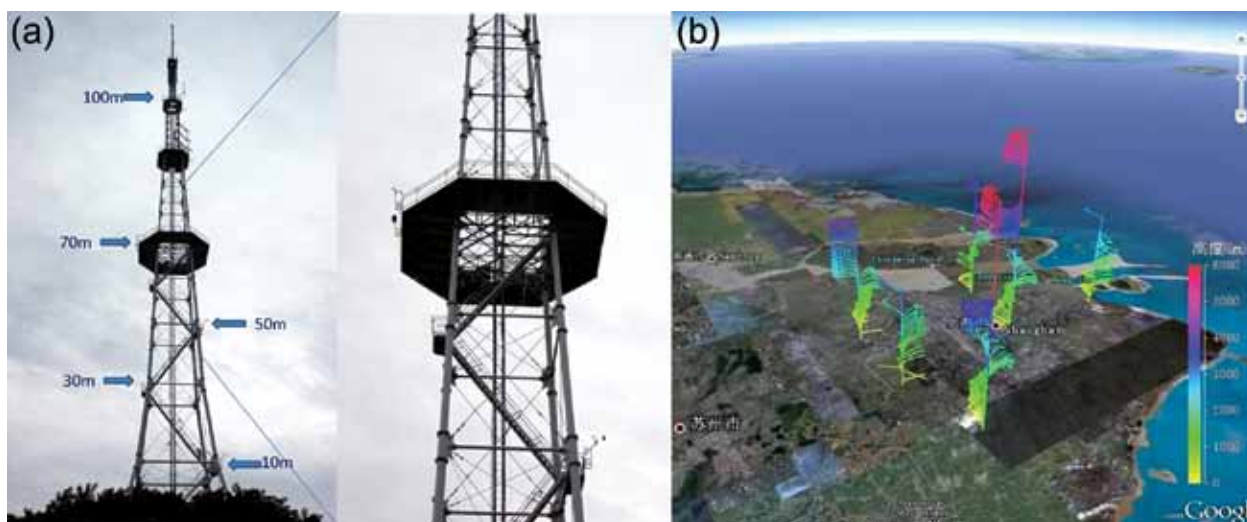
Fig. 2. Information about wind direction and speed with height: (a) instrumented meteorological towers at five levels (Baoshsan tower shown) and (b) wind profilers. Spatial variations on a typical summer day are shown. Color indicates height (0–6000 m); barbs indicate wind speed. Shown on Google Earth base image. See Fig. 1b for locations of both types of sites.

for 24 h are analyzed with a laboratory-based gas chromatography system coupled with mass-selective detection (Geng et al. 2008). Other surface-based in situ observations include particulate matter (PM$_1$, PM$_{2.5}$, PM$_{10}$) and black carbon (BC) (Table 3).

The vertical O$_3$ concentration profile is observed by O$_3$ GPS soundings to understand the exchange between the upper and lower parts of the boundary layer. Other ground-based remote sensing includes lidars [e.g., ceilometers, micropulse (MPL)] and a sun photometer. These provide continuous, real-time measurements of the boundary layer depth and coherent structures by sensing aerosol backscatter (Table 3). MPL data, available from 1 July 2008, allow aerosol extinction coefficients and boundary layer height to be measured with vertical resolution of 30 m from 250 m to 20 km. Column aerosol optical properties and solar extinction, observed with an eight-channel sun photometer during the daytime (Table 3), are used to derive aerosol optical depth (He et al. 2012b). The light scattering coefficient due to particles is measured with an integrating nephelometer.

These data are complemented with those from satellite-based remote sensing [e.g., derived from Moderate Resolution Imaging Spectroradiometer (MODIS), *Feng-Yun-3* (*FY-3*); Table 3] to study the aerosol distribution across Shanghai and east China (He et al. 2012a). Three satellite data receiving systems provide data from eight polar-orbiting [*National Oceanic and Atmospheric Administration-15* (*NOAA-15*)/-16/-17/-18, *FY-3A*, *FY-3B*, Earth Observing System (EOS) *Terra*, and EOS *Aqua*] and four geostationary satellites [*FY-2D*, *FY-2E*, *FY-2F*, and *Multifunctional Transport Satellite 2* (*MTSAT-2*)]. The satellite-derived data are used to monitor a wide range of variables (e.g., cloud location and extent, surface temperature, fog, haze) (Cui and Shi 2010, 2012; Cui et al. 2014).

Data acquisition, integration, and assimilation in SUIMON. Critical to SUIMON is the integrated data management system (DMS) that has been built and operated by the Shanghai Meteorological Service (SMS) (Fig. 3). This acquires and stores the multiscale, multisource meteorological observations (e.g., AWS, weather radars, wind profilers, met tower observations; Table 3) with their metadata (e.g., Table 4). All the information collected at this stage is termed level 0 data.
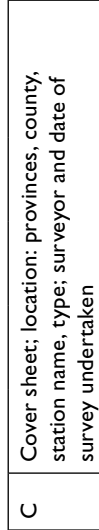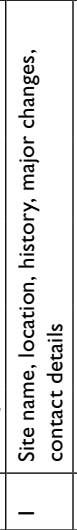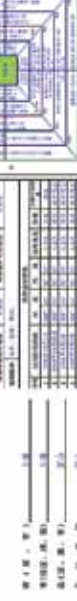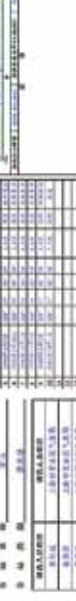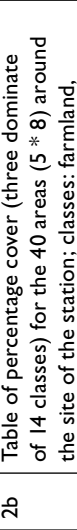
The data undergo initial processing (e.g., decoding, extracting, format checking) and are loaded into raw databases (MySQL/SQL Sever file databases) to create level 1 data. These are stored in a series of different databases (e.g., surface observations, vertical profiler, atmospheric composition).

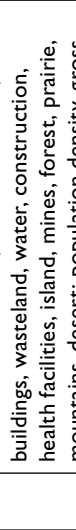The QC subsystem includes an information feedback mechanism to improve the completeness,
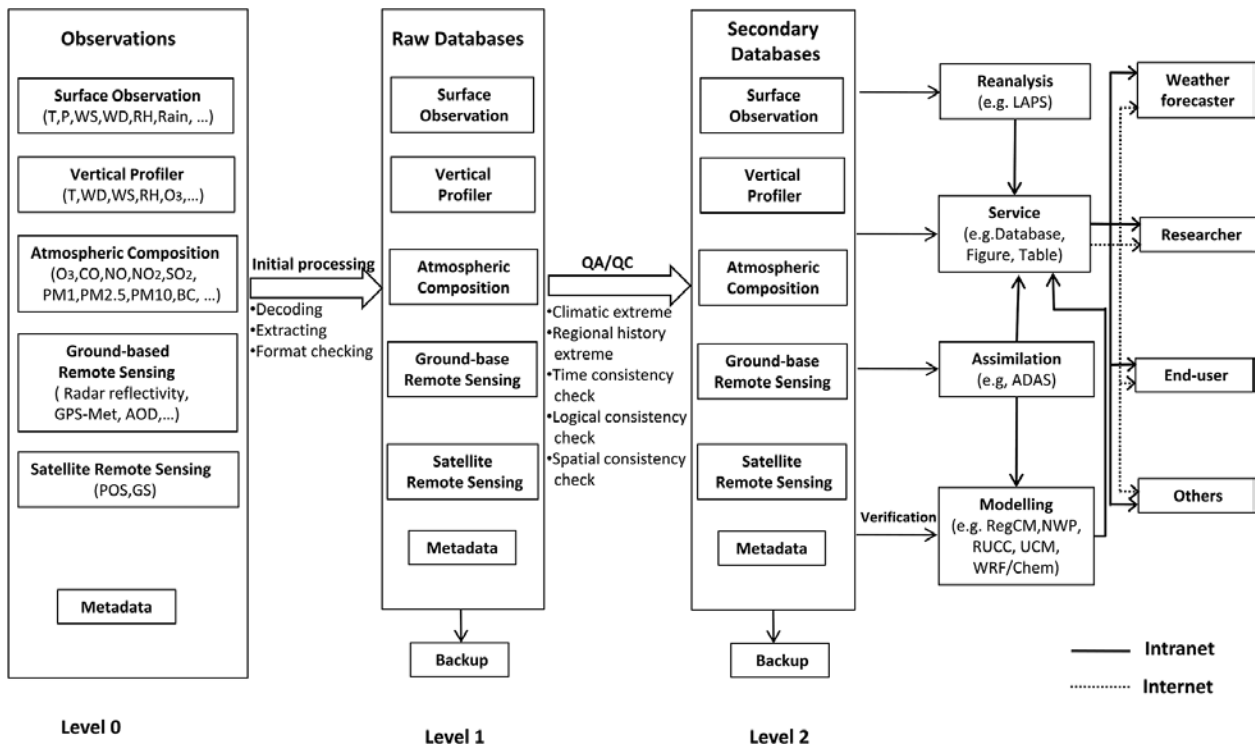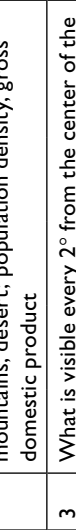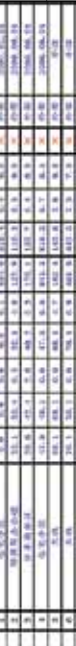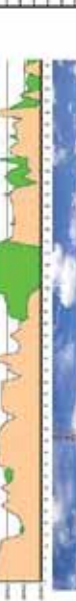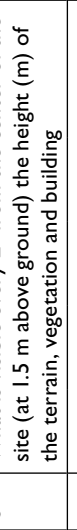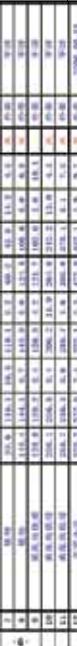

Fɪɢ. 3. Data management and data service of SUIMON.

TABLE 4. Metadata about the site and its surrounding are collected at each site. These data are kept in a digital record (Excel spreadsheet), which allows for consistent and rapid retrieval of data for all sites (automated and manual). The example shown, of 10 pages from the metadata file, is for the Baoshan WMO first-order station for Shanghai. On the left-hand side are images of the individual pages. Top right-hand side provides a key number for the LHS that gives an overview of what is covered in each page shown.

Key	Description
C	Cover sheet; location: provinces, county, station name, type; surveyor and date of survey undertaken
1	Site name, location, history, major changes, contact details
2a	Land cover by distance (5 rings) to the station and direction (8 sectors)
2b	Table of percentage cover (three dominate of 14 classes) for the 40 areas (5 * 8) around the site of the station; classes: farmland, buildings, wasteland, water, construction, health facilities, island, mines, forest, prairie, mountains, desert; population density, gross domestic product
3	What is visible every 2° from the center of the site (at 1.5 m above ground) the height (m) of the terrain, vegetation and building
4	Graph and 360° photo (half shown) of data p. 3
5, 6	Obstacles taller than 1.5 m within 2 km of site
7	Panoramic photo of the site
8	Schematic plan view of a ground station site
9	Aerial photo of the site

C	1	2a	2b	3
4	5			
6	7	8	9	

validity, and accuracy of the meteorological data. The metadata related to the regular instrument calibrations and format are utilized to assess data quality along with monitoring transmission, meteorologically based QC, and comprehensive manual QC. Currently, the QA/QC is performed on the AWS, wind profiler, and met tower data streams automatically by using the approach of both climatic and regional history extremes, a time consistency check, a logical consistency check between variables, and a spatial consistency check. These metrics are used to generate QC flags, which are incorporated into secondary databases with the level 2 data, while the raw databases are kept intact.

The Local Analysis and Prediction System (LAPS) (Liu et al. 2012) and Advanced Regional Prediction System (ARPS) Data Analysis System (ADAS) are used with, and within, SUIMON for integrated data analysis and data assimilation using, for example, the sounding data, AWS, radar reflectivity, wind profiler, and GPS-Met to support mesoscale numerical weather prediction models (NWP). The mesoscale models used include Weather Research and Forecasting (WRF) Model version 3.0. Urban focused observations are used as input or to evaluate submodels for other models such as urban boundary, urban canopy, and air quality models. Different urban land surface schemes such as the Surface Urban Energy and Water Balance Scheme (SUEWS) (Järvi et al. 2011), plus other options with WRF (Chen et al. 2011) and available more generally [e.g., those included in Grimmond et al. (2011)], will be evaluated with SUIMON. The different models are key to the integration of the multiresource nature of the observational data within SUIMON.

For climate modeling, a nested regional climate model developed by the China National Climate Center (RegCM_NCC) (Ding et al. 2006) is used and run operationally in the East China region (green area in Fig. 1 inset). To date, the model performance, evaluated using SUIMON data, has focused on temperature and precipitation (Chen et al. 2008; Dong et al. 2008; Yang et al. 2008). Currently, performance of the Climate extension of the Weather Research and Forecasting Model (CWRF; http://cwrf.umd.edu/) is also being evaluated using SUIMON data for the east China region.

Depending on the requirements, personalized data sharing and services are established for different departments and users. The weather forecasters, researchers, end users, and others receive their required data by means of file transfer protocol (FTP), application programming interface (API), web services, and data pushed through intranet/Internet plus other approaches. Given weather forecasters and researchers within SMS currently are the main users of these observations, their data are available via intranet or Internet. The specialized end users in Shanghai (e.g., transportation sector) get their products (e.g., road weather information) through Internet or point-to-point connection. Different users have different permissions, related to the timeliness, data frequency, and data type that they can access under the regulation on sharing the meteorological observation data to maintain the data securely. International collaborations are encouraged under the framework of bilateral cooperation in meteorological science and technology.

Continuous regular assessment reports are prepared to evaluate the equipment (e.g., AWS, Met towers, weather radars) using indices such as fault time, data acquisition rate, and data errors rate, etc. The data collected regularly to describe the setting for each site are extensive (Table 4), reflecting WMO guidance (Oke 2006) and Muller et al. (2013). These data allow users to assess the characteristics of both individual sensors and the network in terms of applicability for a particular use. The design of individual networks and across networks is reviewed regularly. In addition, as demand from a broader range of sectors for applications has developed, SUIMON as a whole is reviewed to identify how these requests can best be met both with the current configuration plus additional data needs, or personnel with specific skills to support the better use of the data streams.

APPLICATION CASE STUDIES. *Heat island, sea breeze, and convective weather.* Large cities are inherently vulnerable to severe weather such as torrential rain, lightning, and wind gusts. A typical example of the damage caused by torrential rain is inland flooding exacerbated by the large area of impervious surfaces (e.g., asphalt, concrete) and closely spaced buildings of cities. Li et al. (2003) developed a fine-mesh regional meteorological model that has been applied in Shanghai and neighboring areas to simulate small-scale weather features, such as the land and sea breeze, land and lake breezes, and UHI effect in this area and to study the characteristics and the formation mechanism of the surface shear line in the region. The results suggest that the interaction between the sea breeze and the lake breeze is the main factor for the formation and maintenance of the surface shear line that is related to the short-term convective weather. Based on the dense meteorological observation network in SUIMON, the distribution

of occurrence of the severe convective precipitation events (daily rainfall > 50 mm) derived from the dense surface AWS monitoring records (Fig. 4a) shows a high frequency over the urban area and the mouth of the Yangtze River that matches well with the spatial distribution of cloud-to-ground flash density (Fig. 4b). This may be due to the presence of the urban heat island and the sea breeze circulation. For example, on 15 August 2012 (Fig. 5) there was a short period of convective precipitation that fell on the northwestern part of the Shanghai area. Prior to this there was both an UHI (2-m air temperatures) and a sea breeze. These combined to create two areas of convergence and areas of surface wind shear (Fig. 5).

SUIMON has, and is being, used to investigate UHI effects on thermodynamic instability, UHI convergence in association with intensification and/or initiation of electrically active thunderstorms in the metropolitan area, and UHI enhancement of convective updraft strength in relation to the frequency of lightning. This is helping to characterize and evaluate thermodynamic and kinematic structures of thunderstorms, in the context of a better knowledge of the physical process of rain formation, maintenance and evolution. For example, a large hail-producing supercell developed ahead of a severe squall line around Shanghai on 5 June 2009. The supercell and its interaction and relations with the squall line over the urban environment were analyzed using a number of SUIMON data sources including the AWS network, Doppler radar, and wind profiler data (Dai et al. 2012).

The data analysis revealed that the storm intensified while passing through a surface convergence zone induced jointly by the UHI and a sea breeze front. Techniques such as quantitative precipitation estimation (QPE) and quantitative precipitation forecasts (QPFs) have been developed, improved, and employed in operational applications to assess the urban waterlogging risk under rainfall condition in Shanghai (Zou et al. 2012). Knowledge that the most vulnerable areas are in the urban center and mouth of the Yangtze River can now be correlated with exposure (e.g., socioeconomic, construction, industrial activities) in these areas to develop risk maps for improving emergency preparedness.

Photochemical and urban aerosol pollution. Cities are a major source of air pollution emissions owing to the burning of fossil fuels for heating and cooling, industrial processing, and transport of people and goods. Cities also modify their ambient weather (especially winds, turbulence, radiation, mixing height, and temperature) in ways that often negatively affect the dispersion, transformation, and concentration of those pollutants. Air quality forecasts and warnings are needed at multiple scales of the region, city, and street. Information about the atmospheric circulation are combined with the higher temporal-, vertical-, and horizontal spatial-resolution data (e.g., urban boundary layer structure and mixing layer heights, vertical profiles of winds, turbulence, temperature inversion). The city, with its characteristic
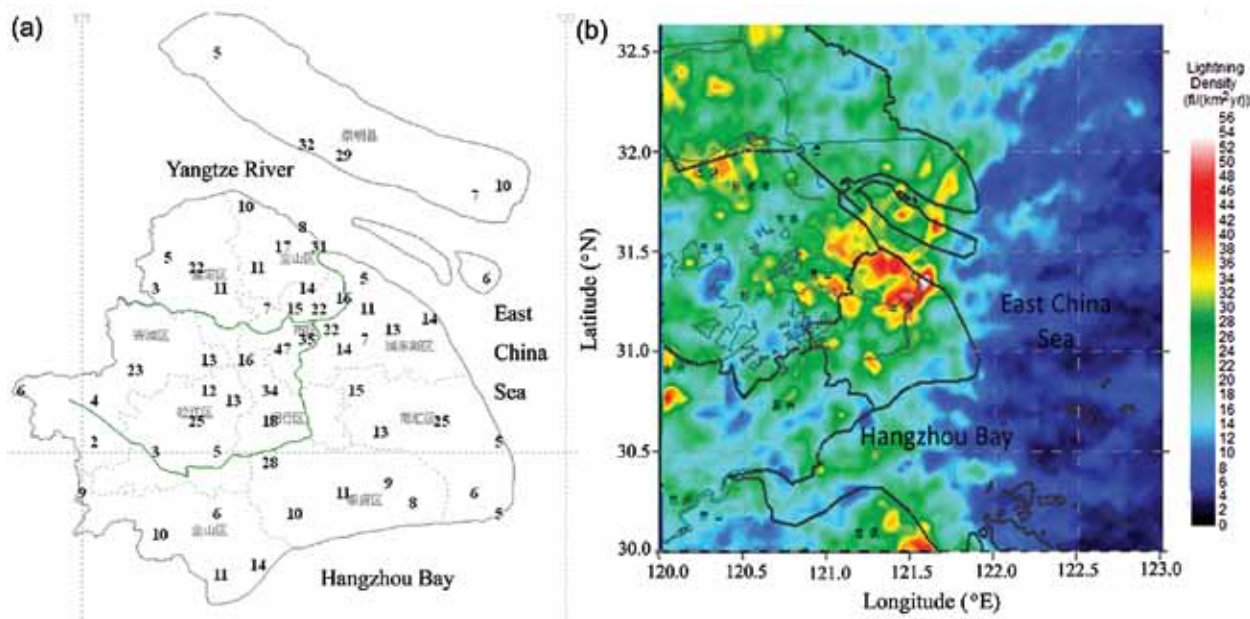

FIG. 4. (a) Number of severe convective precipitation events (1994–2008) and (b) spatial distribution of cloud-to-ground flash density (flashes yr^{-1} km^{-2}) (2008–12).

roughness height and temperature evolution, has a strong impact on the structure of the urban boundary layer and hence on the pollutant dispersion near the surface.

Within SUIMON, O_3 concentration and photochemical precursors have been systemically measured and their relations investigated (Geng et al. 2007; Ran et al. 2009). For example, the ozone "weekend effect" (Tang et al. 2008) and the impacts of the precursors on ozone formation (Geng et al. 2008) have been revealed.

Ground-based remote sensing [e.g., sun photometer, micropulse lidar version 4 (MPL 4), ceilometer] have been used to investigate urban aerosol and fog/haze events (Huang et al. 2010; He et al. 2012a,b). The observations have been used to evaluate the performance of the WRF-Chem Model. This is now used routinely for the chemical weather forecast for the Yangtze River delta region (Zhou et al. 2012). Furthermore, SUIMON is being used to improve the chemical weather forecast by providing improved data for a reaction scheme of photooxidants and particle interactions. This has been taken further to investigate the relation between air pollution and human health (Cao et al. 2009; Huang et al. 2009; Chen et al. 2010).
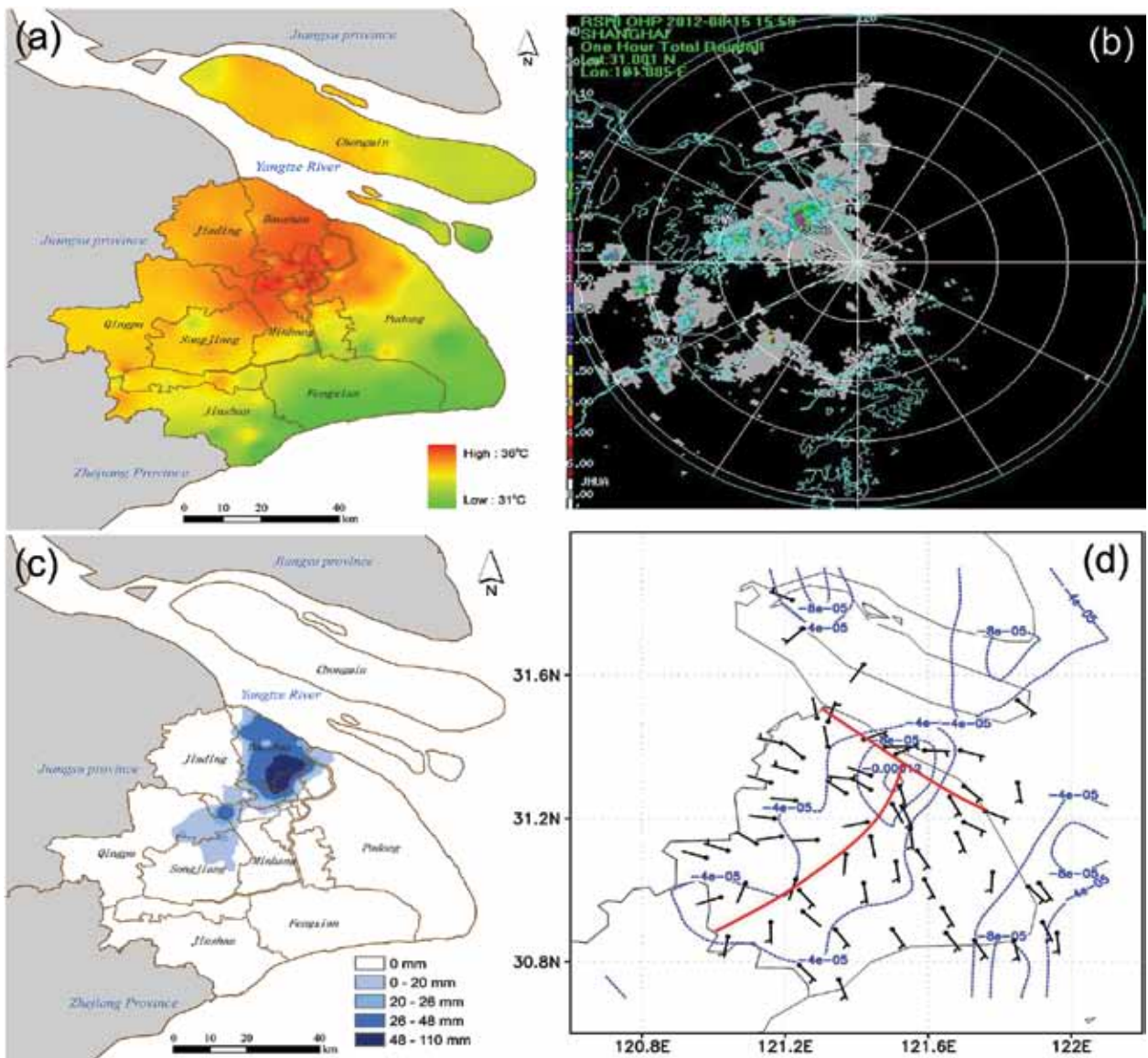
Fig. 5. Short-term convective precipitation associated with urban heat island and sea breeze convergence lines on 15 Aug 2012 (a) accumulated rainfall distribution between 1300 and 1700 LST measured by AWS and rain gauges, (b) radar OHP (one-hour total rainfall) before 1559 LST, (c) air temperature distribution at 2 m measured by AWS on 1200 LST, and (d) wind speed and direction at 10 m at 1200 LST and the two surface wind shear lines (red); blue lines indicate the surface convergence zone.

End user applications supported by SUIMON. The SUIMON data are provided in near–real time to weather forecasters. The publically accessible website (www.soweather.com/index.html) provides weather forecast/warnings, plus more specialized forecasts, such as for road and health. With the aid of a geographic information system (GIS) interface the public can access the real-time Met records and forecasts for the area of the city of interest to them. New specialized products are being developed in conjunction

| TABLE 5. Examples of urban weather/climate and environmental services in Shanghai.		
Sectors	Examples of urban weather/climate and environmental services	End users (examples)
Water	River catchment precipitation Urban inundation Coastal storm surges	Water authority, emergency response center, drainage company
Urban infrastructure	Urban wind, heavy rainfall, heat wave, lightning forecast	Urban planning bureau, urban green bureau, public
Energy	Wind and solar resource assessment Wind power forecast for wind mill Energy consumption estimation (electric, gas)	Development and reform commission, power companies, wind power plants
Health	UV index Pollen concentration Heat/health warnings Weather-/climatic-based disease prediction [asthma, chronic obstructive pulmonary disease (COPD)]	Public health authority, public
Environment	Air quality index (AQI) forecast Haze, O_3 forecast NBC release	Environment protection bureau, hospitals, schools, public
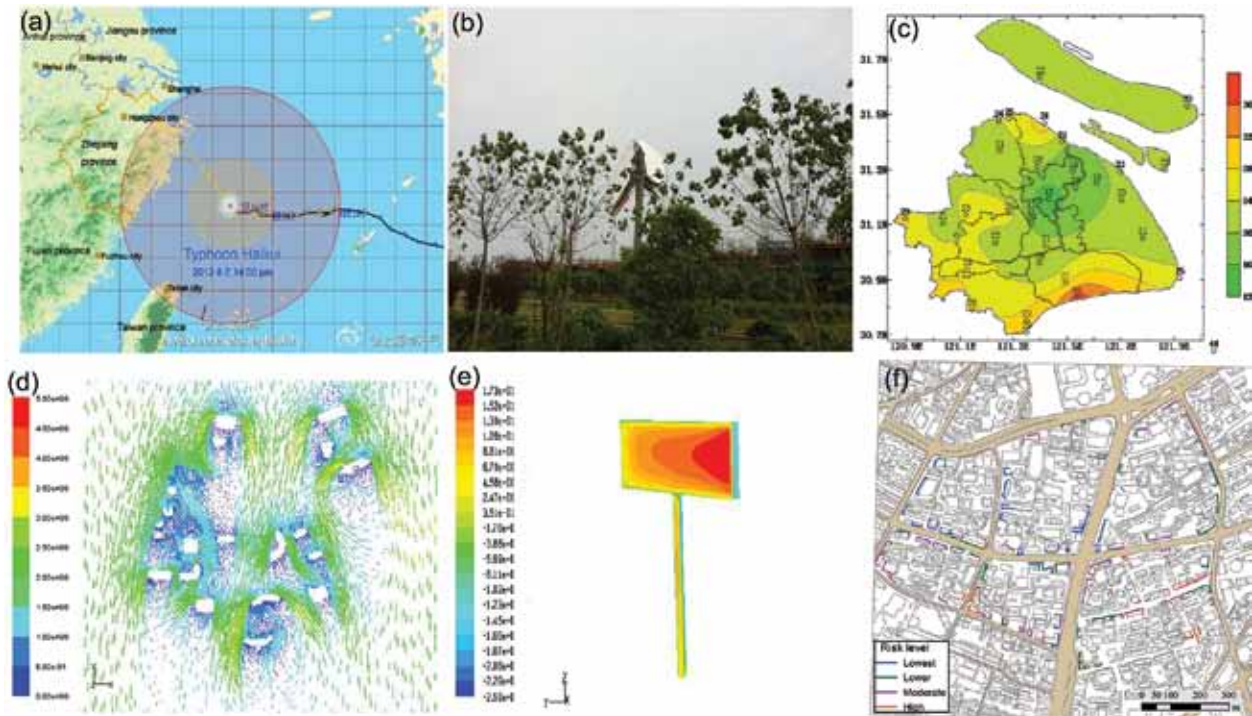
FIG. 6. Typhoon Haikuion 7 Aug 2012 (a) track and intensity was monitored, forecasted, and warnings delivered to the public. The storm caused damage in the area. (b) One type of damage that occurs frequently is the collapse of billboards. Example shown from a highway in Shanghai during Typhoon Haikui. (c) The maximum wind speed (m s^{-1}) across the whole Shanghai area monitored at 10 m. (d) Detailed analysis undertaken on billboard design and siting to enhance public safety so the area is better prepared for future typhoons. Analysis conducted using the Fluent CFD model to estimate the canopy wind distribution (m s^{-1}), (e) wind load on billboard (N m^{-2}), and (f) different risk levels caused by the gusts on billboards along major roads.

with end users—for example, urban inundation warnings, meteorological condition forecasts to aid safe driving, energy demand, and related loads on the electric grid (Table 5).

One impetus for enhancing the density of data collection near the city center was the World Exposition (Expo) held in Shanghai during the summer of 2010. During that time an even denser network of sensors (area 5.28 km^2) was embedded in SUIMON. These provided real-time support for improved high risk weather prediction for the region, down to detailed knowledge across the Expo park for heat exposure (Tang et al. 2012).

New specialized forecasts are being developed for different sectors. For example, with the building of the Shanghai Tower (632 m, one of the tallest buildings in the world) and other large construction projects, the ability to forecast winds at more than 100 m above the surface becomes critical both for those involved in construction and those working/living in the vicinity (Fang et al. 2013). This has taken advantage of SUIMON wind profiler data and the met towers more directly, but also other data feeds have been used to enhance the data assimilation into the NWP model generally.

Given the high frequency of intense storms, the design of billboards that are permitted in the city has become one area of focus given the damage caused when intense gusts cause them to become unattached (Fig. 6b). Combining Fluent computational fluid dynamics (CFD) modeling (Fang et al. 2013), with the extensive wind data available across the area, has resulted in new designs to reduce damage (Figs. 6d,e). Combining these with risk assessment, this information is intended to inform planning to identify areas that are likely to be better and poorer choices for installing different types of billboards (Fig. 6f).

FUTURE CONSIDERATIONS IN URBAN METEOROLOGICAL OBSERVATIONS IN SHANGHAI.
In the next five years, to meet emerging science- and user-driven needs and requirements, the Shanghai Meteorological Service (SMS) expects to enhance the multifunctions of Shanghai's Urban Integrated Meteorological Observation Network (SUIMON). The emphasis will be on the acquisition of information associated with physical processes of the urban boundary layer and the effects of the underlying surface (see "Future enhancements to SUIMON" for more information). It is expected that SUIMON will continue to evolve because of new user requests and new technologies, as it repeatedly has done over

FUTURE ENHANCEMENTS TO SUIMON

- Meso- and microscale processes over urban surfaces (such as cloud microphysics, precipitation processes)
- Height (and structure) of the PBL and vertical profiles of wind, temperature, water vapor, and atmospheric composition
- Field studies to validate satellite observations and modeling simulations of urban precipitation processes and to extend basic understanding of the processes involved
- Enhancing existing observing systems to focus on city–atmosphere interactions, especially to monitor and track land-cover/land-use changes, atmospheric composition, cloud microphysics, and precipitation processes
- Modeling systems that explicitly resolve multiscale (e.g., urban canopy, street, building) processes, aerosols and cloud microphysics, and complex land surfaces to enable a more complete understanding of the feedbacks and interactions

the last 140 years. Many of the developments in the near future are expected to involve better use of the combined database. One key challenge is how to monitor the spaces between buildings given the rapid increase in tall buildings (Table 2) in Shanghai and the many other rapidly growing cities of Asia and South America. Applications from response to fires to management of energy use to near-surface air quality would benefit from improved understanding of this very large urban canopy layer.

SUIMON, with measurements to end user support provides a prototype for integrated urban weather, environment, and climate services as suggested by Grimmond et al. (2014).

REFERENCES

Allwine, K. J., J. H. Shinn, G. E. Streit, K. L. Clawson, and M. J. Brown, 2002: Overview of Urban 2000: A multiscale field study of dispersion through an urban environment. *Bull. Amer. Meteor. Soc.,* **83,** 521–536, doi:10.1175/1520-0477(2002)0832.3.CO;2.

——, M. J. Leach, L. W. Stockham, J. S. Shinn, J. F. Bowers, and J. C. Pace, 2004: Overview of Joint Urban 2003: An atmospheric dispersion study in Oklahoma City. *Eighth Symp. on Integrated Observing and Assimilation Systems in the Atmosphere, Oceans, and Land Surface* and *Symp. on Planning, Nowcasting, and Forecasting in the Urban Zone,* Seattle, WA, Amer. Meteor. Soc., J7.1. [Available online at https://ams.confex.com/ams/84Annual/techprogram/paper_74349.htm.]

Arnold, S. J., and Coauthors, 2004: Introduction to the DAPPLE air pollution project. *Sci. Total Environ.,* **332,** 139–153, doi:10.1016/j.scitotenv.2004.04.020.

Aubinet, M., T. Vesala, and D. Papale, Eds., 2012: *Eddy Covariance: A Practical Guide to Measurement and Data Analysis.* Springer Atmospheric Sciences, 438 pp.

Bohnenstengel S. I., and Coauthors, 2015: Meteorology, air quality, and health in London: The ClearfLo project. *Bull. Amer. Meteor. Soc.,* in press, doi:10.1175/BAMS-D-12-00245.1.

Cao, J. S., and Coauthors, 2009: Association of ambient air pollution with hospital outpatient and emergency room visits in Shanghai, China. *Sci. Total Environ.,* **407,** 5531–5536, doi:10.1016/j.scitotenv.2009.07.021.

Chen, B. M., Y. W. Yang, G. T. Dong, Y. M. Liu, Z. Z. Wang, and T. W. Wu, 2008: An application of regional climate model (RegCM_NCC) in operation over the East China (I): A real-time run from December 2007 to February 2008 and hindcasting experiments (in Chinese). *Plateau Meteor.,* **27** (Suppl.), 22–31.

Chen, F., and Coauthors, 2011: The integrated WRF/urban modelling system: Development, evaluation, and applications to urban environmental problems. *Int. J. Climatol.,* **31,** 273–288, doi:10.1002/joc.2158.

Chen, R. J., and Coauthors, 2010: Ambient air pollution and hospital admission in Shanghai, China. *J. Hazard. Mater.,* **181,** 234–240, doi:10.1016/j.jhazmat.2010.05.002.

Cros, B., and Coauthors, 2004: The ESCOMPTE program: An overview. *Atmos. Res.,* **69,** 241–279, doi:10.1016/j.atmosres.2003.05.001.

Cui, L. L., and J. Shi, 2010: Temporal and spatial response of vegetation NDVI to temperature and precipitation in eastern China. *J. Geogr. Sci.,* **20,** 163–176, doi:10.1007/s11442-010-0163-4.

——, and ——, 2012: Urbanization and its environmental effects in Shanghai, China. *Urban Climate,* **2,** 1–15, doi:10.1016/j.uclim.2012.10.008.

——, L. H. Shi, Q. Yin, W. Yu, X. Q. Lu, and J. Liu, 2014: Application of satellite cloud imagery in track analysis of tropical cyclones. *Trop. Cyclone Res. Rev.,* **2,** 222–232.

Dabberdt, W. F., 2012: Urban meteorological measurements. *Urban Meteorology: Forecasting, Monitoring, and Meeting Users' Needs,* National Academies Press, Committee on Urban Meteorology: Scoping the Problem, Defining the Needs et al., 137–148. [Available online at www.nap.edu/catalog.php?record_id=13328.]

——, J. Koistinen, J. Poutiainen, E. Saltikoff, and H. Turtianinen, 2005: The Helsinki Mesoscale Testbed: An invitation to use a new 3-D observation network. *Bull. Amer. Meteor. Soc.,* **86,** 906–907, doi:10.1175/BAMS-86-7-906.

Dai, J. H., L. Tao, Y. Ding, Y. Wang, and L. Chen, 2012: Case analysis of a large hail-producing severe supercell ahead of a squall line (in Chinese). *Acta Meteor. Sin.,* **70,** 609–627.

Ding, Y. H., and Coauthors, 2006: Multi-year simulations and experimental seasonal predictions for rainy seasons in China by using a nested regional climate model (RegCM-NCC). Part I: Sensitivity study. *Adv. Atmos. Sci.,* **23,** 323–341, doi:10.1007/s00376-006-0323-8.

Dong, G. T., B. M. Chen, and Y. W. Yang, 2008: An application of regional climate model (RegCM_NCC) in operation over the East China (III): 10-year hindcast experiments of spring and autumn (in Chinese). *Plateau Meteor.,* **27** (Suppl.), 42–51.

Fang, P. Z., J. Shi, Q. Wang, Z. H. Hang, and J. G. Tan, 2013: Numerical study on wind environment among tall buildings in Shanghai Lujiazui Zone (in Chinese). *J. Build. Struct.,* **34,** 104–111.

Geng, F. H., C. S. Zhao, X. Tang, G. L. Lu, and X. X. Tie, 2007: Analysis of ozone and VOCs measured in Shanghai: A case study. *Atmos. Environ.,* **41,** 989–1001, doi:10.1016/j.atmosenv.2006.09.023.

——, X. X. Tie, J. M. Xu, G. Q. Zhou, L. Peng, W. Gao, X. Tang, and C. S. Zhao, 2008: Characterizations of ozone, NOx, and VOCs measured in Shanghai, China. *Atmos. Environ.,* **42,** 6873–6883, doi:10.1016/j.atmosenv.2008.05.045.

Gherzi, E., 1950: The scientific work of the Catholic Church at the Zikawei Observatory in Shanghai. *Bol. Inst. Port. Hong Kong,* **3,** 45–47.

Grimmond, C. S. B., and Coauthors, 2010: Climate and more sustainable cities: Climate information for improved planning and management of cities (producers/capabilities perspective). *Procedia Environ. Sci.,* **1,** 247–274, doi:10.1016/j.proenv.2010.09.016.

——, and Coauthors, 2011: Initial results from phase 2 of the International Urban Energy Balance Comparison Project. *Int. J. Climatol.,* **31,** 244–272, doi:10.1002/joc.2227.

——, X. Tang, and A. Baklanov, 2014: Towards integrated urban weather, environment and climate services.

WMO Bull., **63,** 10–14. [Available online at www.wmo .int/pages/publications/bulletin_en/Bulletin631 -2014_TowardsIntegratedUrbanWeather_en.html.]

Hanna, S. R., J. White, Y. Zhou, and A. Kosheleva, 2006: Analysis of Joint Urban 2003 (JU2003) and Madison Square Garden 2005 (MSG05) meteorological and tracer data. *Sixth Symp. on the Urban Environment,* Atlanta, GA, Amer. Meteor. Soc., J7.1. [Available online at https://ams.confex.com/ams/Annual2006 /techprogram/paper_104131.htm.]

Harrison, R. M., and Coauthors, 2012: Atmospheric chemistry and physics in the atmosphere of a developed megacity (London): An overview of the REPARTEE experiment and its conclusions. *Atmos. Chem. Phys.,* **12,** 3065–3114, doi:10.5194/acp-12 -3065-2012.

He, Q. S., C. C. Li, F. H. Geng, Y. Lei, and Y. H. Li, 2012a: Study on long-term aerosol distribution over the land of East China using MODIS Data. *Aerosol Air Qual. Res.,* **12,** 304–319.

——, ——, ——, H. Q. Yang, P. R. Li, T. T. Li, D. W. Liu, and Z. Pei, 2012b: Aerosol optical properties retrieved from sun photometer measurements over Shanghai, China. *J. Geophys. Res.,* **117,** D16204, doi:10.1029/2011JD017220.

Hicks, B. B., W. J. Callahan, W. R. Pendergrass III, R. J. Dobosy, and E. Novakovskaia, 2012: Urban turbulence in space and time. *Bull. Amer. Meteor. Soc.,* **51,** 205–218, doi:10.1175/JAMC-D-11-015.1.

Huang, W., and Coauthors, 2009: Visibility, air quality and daily mortality in Shanghai, China. *Sci. Total Environ.,* **407,** 3295–3300, doi:10.1016/j .scitotenv.2009.02.019.

Huang, X. Y., X. W. Yang, F. H. Geng, H. Zhang, Q. S. He, and L. B. Bu, 2010: Aerosol measurement and property analysis based on data collected by a micropulse LIDAR over Shanghai, China. *J. Opt. Soc. Korea,* **14,** 185–189, doi:10.3807/JOSK.2010.14.3.185.

Järvi, L., C. S. B. Grimmond, and A. Christen, 2011: The Surface Urban Energy and Water Balance Scheme (SUEWS): Evaluation in Vancouver and Los Angeles. *J. Hydrol.,* **411,** 219–237, doi:10.1016/j .jhydrol.2011.10.001.

Koskinen, J. T., and Coauthors, 2011: The Helsinki Testbed: A mesoscale measurement, research, and service platform. *Bull. Amer. Meteor. Soc.,* **92,** 325–342, doi:10.1175/2010BAMS2878.1.

Li, W. L., H. L. Liu, X. J. Zhou, and Y. Qin, 2003: Analysis of the influence of Taihu Lake and the urban heat island on the local circulation in the Yangtze Delta. *Sci. China,* **46D,** 405–415.

Liang, X. D., 2007: An integrating velocity–azimuth process single-Doppler radar wind retrieval method. *J. Atmos. Oceanic Technol.,* **24,** 658–665, doi:10.1175 /JTECH2047.1.

Liu, S. D., Y. Q. Tang, L. L. Shao, and H. Y. Liu, 2012: The application of LAPS products in mesoscale analysis of a severe storm (in Chinese). *J. Nanjing Inst. Meteor.,* **35,** 391–403.

Maki, M., and Coauthors, 2012: Tokyo Metropolitan Area Convection Study for Extreme Weather Resilient Cities (TOMACS). *Extended Abstracts, Seventh European Conf. on Radar in Meteorology and Hydrology,* Toulouse, France. [Available online at www.meteo.fr/cic/meetings/2012/ERAD /extended_abs/NET_236_ext_abs.pdf.]

Masson, V., and Coauthors, 2008: The Canopy and Aerosol Particles Interactions in Toulouse Urban Layer (CAPITOUL) experiment. *Meteor. Atmos. Phys.,* **102,** 135–157, doi:10.1007/s00703-008-0289-4.

Muller, C. L., L. Chapman, C. S. B. Grimmond, D. T. Young, and X. M. Cai, 2013: Toward a standardized metadata protocol for urban meteorological networks. *Bull. Amer. Meteor. Soc.,* **94,** 1161–1185, doi:10.1175/BAMS-D-12-00096.1.

National Research Council, 2010: *When Weather Matters: Science and Service to Meet Critical Societal Needs.* National Academies Press, 198 pp. [Available online at www.nap.edu/openbook.php?record _id=12888.]

——, 2012: *Urban Meteorology: Forecasting, Monitoring, and Meeting Users' Needs.* National Academies Press, 190 pp. [Available online at www.nap.edu/openbook .php?record_id=13328.]

Oke, T. R., 2006: Initial guidance to obtain representative meteorological observation at urban sites, Instruments and observing methods. WMO Tech. Rep. 81, 1–47. [Available online at http://library.wmo.int/opac/index .php?lvl=notice_display&id=9262#.VIM6QjGsVps.]

Orville, R., R. Zhang, J. Nielsen-Gammon, D. Collins, B. Ely, and S. Steiger, 2004: Houston Environmental Aerosol Thunderstorm (HEAT) project. Texas A&M University Department of Atmospheric Sciences, 57 pp. [Available online at http://atmo.tamu.edu/ciams /heat/HEAT_plan.pdf.]

Ran, L., and Coauthors, 2009: Ozone photochemical production in urban Shanghai, China: Analysis based on ground level observations. *J. Geophys. Res.,* **114,** D15301, doi:10.1029/2008JD010752.

Reynolds, R. M., cited 2014: UAO: Urban Atmospheric Observatory: Instrumentation network verification facility - New York City. [Available online at www.bnl.gov/uao/.]

Rotach, M. W., and Coauthors, 2005: BUBBLE—An urban boundary layer meteorology project. *Theor. Appl. Climatol.,* **81,** 231–261, doi:10.1007/s00704 -004-0117-9.

Shanghai Statistics Bureau, cited 2014: Shanghai statistical yearbook 2012. [Available online at www.stats-sh.gov.cn/.]

Takahashi, K., T. Mikami, and H. Takahashi, 2009: Influence of the urban heat island phenomenon in Tokyo in land and sea breezes. *Extended Abstracts, Seventh Int. Conf. on Urban Climate,* Yokohama, Japan, IAUC, P1-14. [Available online at www.ide.titech.ac.jp/~icuc7/extended_abstracts/pdf/384122-1-090518113435-004.pdf.]

Tang, W. Y., C. S. Zhao, F. H. Geng, L. Peng, G. Q. Zhou, W. Gao, J. M. Xu, and X. X. Tie, 2008: Study of ozone "weekend effect" in Shanghai. *Sci. China,* **51D,** 1354–1360, doi:10.1007/s11430-008-0088-2.

Tang, X., 2008: New challenges for weather services in changing urban environment. *WMO Bull.,* **57,** 244–248. [Available online at www.wmo.int/pages/publications/bulletin_en/archive/57_4_en/documents/57_4_tang_sub_en.pdf.]

——, L. Feng, Y. Zou, and H. Mu, 2012: The Shanghai Multi-Hazard Early Warning System: Addressing the challenge of disaster risk reduction in an urban megalopolis. *Institutional Partnerships in Multi-Hazard Early Warning Systems,* M. Golnaraghi, Ed., Springer Berlin Heidelberg, 159–179.

United Nations, 2013: World population prospects: The 2012 revision, key findings and advance tables. United Nations Department of Economic and Social Affairs/Population Division Working Paper ESA/P/WP.227, 50 pp. [Available online at http://esa.un.org/unpd/wpp/Documentation/pdf/WPP2012_%20KEY%20FINDINGS.pdf.]

Warner, T., and Coauthors, 2007: The Pentagon Shield Field Program: Toward critical infrastructure protection. *Bull. Amer. Meteor. Soc.,* **88,** 167–176, doi:10.1175/BAMS-88-2-167.

WMO, 1996: Guide to meteorological instruments and methods of observation. 7th ed. World Meteorological Organization Rep. WMO 8, 680 pp. [Available online at www.wmo.int/pages/prog/gcos/documents/gruanmanuals/CIMO/CIMO_Guide-7th_Edition-2008.pdf.]

Yang, Y. W., B. M. Chen, G. T. Dong, and G. L. Zhong, 2008: An application of regional climate model (RegCM_NCC) in operation over the East China (II): 10-year summertime hindcasts (in Chinese). *Plateau Meteor.,* **27** (Suppl.), 32–41.

Zhou, G. Q., L. Peng, F. H. Geng, J. M. Xu, F. Yang, and X. X. Tie, 2012: Chemical weather forecast over the Yangtze River Delta Region: Application of WRF-Chem. *Symp. on Robotics and Applications (ISRA),* Kuala Lumpur, Malaysia, IEEE, 793–796, doi:10.1109/ISRA.2012.6219310.

Zhou, S. Z., and S. D. Chow, 1990: 5 islands effects of Shanghai urban climate. *Sci. China,* **33B,** 67–78.

——, S. D. Chow, and J. C. Zheng, 1991: The turbidity island effect in Shanghai urban climate. *Energy Build.,* **16,** 657–662, doi:10.1016/0378-7788(91)90034-Z.

Zou, L. J., Z. Wang, and Y. M. Yang, 2012: Assessing the urban waterlogging risk under rainfall condition in Shanghai. *Extended abstracts, 16th Int. Road Weather Conf.,* Helsinki, Finland, SIRWEC, ID0080. [Available online at www.sirwec2012.fi/Extended_Abstracts/080_Zou.pdf.]

Zou, X. J., 2011: Analysis of population movement and distribution based on Sixth Census (in Chinese). *Popul. Econ.,* **6,** 24–33.